Transplantation of Neuregulin1-Overexpressing Bone Marrow Mesenchymal Cells Accelerates Motor Functional Recovery by Facilitating Neurite Outgrowth and Reducing Cell Apoptosis in Rat after Spinal Cord Injury

Geng Wu
Mudanjiang Medical University
Herui Liu
Mudanjiang Medical University
Mei Zhu
Mudanjiang Medical University
Yang Wu
Mudanjiang Medical University
Yunlong Bai
Jiamusi University
Yan Liu
Mudanjiang Medical University
Jinfeng Wang
Mudanjiang Medical University
Jianbo Yu
Mudanjiang Medical University
Fusheng Zhao (zhaofusheng@mdjmu.edu.cn)
Mudanjiang Medical University

Research

Keywords: Neuregulin1, Bone marrow mesenchymal stem cells, Spinal cord injury, Neurite outgrowth, Apoptosis

Posted Date: August 31st, 2020

DOI: https://doi.org/10.21203/rs.3.rs-67905/v1

Abstract

Background: Bone marrow mesenchymal stem cells (BMSCs) transplantation offers an attractive strategy for treating multiply neurological diseases. Neuregulin1 (NRG1) plays fundamental roles in nervous system development and nerve repair. In this study, we aimed to investigate whether transplantation of NRG1-overexpressing BMSCs could alleviate spinal cord injury (SCI), and to explore the possible underling mechanisms.

Methods: *In vitro*, NRG1-overexpressing BMSCs were constructed via plasmid transfection, and co-cultured with PC12 cells subjected to oxygen-glucose deprivation (OGD). Neurite outgrowth, cell viability and apoptosis of PC12 cells were evaluated. *In vivo*, BMSCs, empty-vector BMSCs and NRG1-overexpressing BMSCs were transplanted respectively into rats with SCI. Rat locomotor functions, neuronal chromatolysis, neurite outgrowth and cell apoptosis were assessed respectively.

Results: The results showed that NRG1-overexpressing BMSCs *in vitro* significantly expedited neurite growth, elevated growth-associated protein 43 expression, enhanced cell viability and rescued ODG-induced apoptosis in PC12 cells. *In vivo*, transplantation of NRG1-overexpressing BMSCs notably accelerated rat motor functional recovery, attenuated neuronal chromatolysis, promoted neurite outgrowth and reduced cell apoptosis after SCI. Moreover, NRG1-overexpressing BMSCs were also able to regulate apoptosis-related proteins expression after SCI.

Conclusions: These findings demonstrate that NRG1-overexpressing BMSCs can accelerate motor functional recovery by facilitating neurite outgrowth and reducing cell apoptosis after SCI, suggesting that NRG1-overexpressing BMSCs may be a promising candidate for the treatment of SCI.

Background

Spinal cord injury (SCI) occurs with a worldwide annual incidence of 10.4–83 cases per million people, and it remains a major public health issue [1]. The mortality of acute SCI is between 48 and 79%, and the survivors present more often with a range of functional impairments, including sensory, motor and autonomic dysfunction [2]. The pathology of SCI can be divided into two stages: the primary injury that is the initial mechanical damage; and the secondary injury that starts after primary insult and involves a series of biochemical alterations, such as local hemorrhage, oxidative stress, inflammation, the disturbances of ionic homeostasis, axonal disruption as well as neuronal and glial apoptosis, which spread beyond the initial injury site and result in irreversible paraplegia and quadriplegia [3]. Despite substantial efforts, there are yet no effective therapies for SCI beyond early surgical decompression, stabilization, as well as aggressive supportive care.

In recent decades, many different types of stem cell, including embryonic stem cells [4], neural stem cells [5], olfactory ensheathing cells [6], Schwann cells [7] and stem cells from non-neural tissues such as bone marrow mesenchymal stem cells (BMSCs) [8], have been used for treatment of SCI, and the cellular events that occur in SCI have been studied in a variety of animal models. Relative to embryonic stem cells

or other stem cells, BMSCs have become the favorite seed cells in the preclinical and clinical practice due to their properties of low immunogenicity, wide biological effects, and lack of ethical problems [3]. In addition, BMSCs can be easily isolated, expanded, genetically modified, and stably expressed exogenous genes [9]. BMSCs also exhibit the advantage of being autologous, and have the potential to differentiate into non-mesodermal cell types such as neurons [10]. Moreover, there is evidence that BMSCs can attenuate the pathological changes that arise after the stroke [11], and promote myelinization in a rat model of middle cerebral artery occlusion [12].

Neuregulin1 (NRG1), a member of the NRG family, is a type of signal protein encoded by the NRG1 gene [13]. NRG1 can be classified into three major types (I, II, and III) based on the type of amino-terminal sequence, and further characterized as type α or β according to the features of the epidermal growth factor (EGF)-like domain [14, 15]. All three types of NRG1 proteins share high-sequence homology in their EGF-like domain, which is sufficient to bind their cognate receptors, members of the ErbB family, and activate downstream signaling pathways [16]. The evidence indicates that NRG1 has involved in many cellular biological processes, such as cell proliferation, differentiation, and migration [17]. In the central nervous system (CNS), NRG1 expresses in migrating neurons and oligodendrocyte precursors, and is thought to positively influence oligodendrocyte development and radial glial cell function [18]. Additionally, NRG1 also affects dendritic spine maturation and synapse formation in the CNS [19]. In the peripheral nervous system, NRG1 plays a critical role in axon myelination, and influences the survival and migration of Schwann cell precursors [20]. There is evidence that NRG1 can facilitate myelin formation and improve the recovery of injured nerves [21]. Studies from our laboratory indicated that NRG1 exerted neuroprotective effects against SCI by reducing spinal cord histological damage, and promoting axonal regeneration in rats [22–24]. Some studies reported that NRG1 was capable of preserving endothelial barrier function, and reducing BBB permeability in traumatic brain injury [25, 26].

Taking into account the features of BMSCs and biological functions of NRG1, we therefore modified BMSCs in this study with NRG1 gene, and defined the role of NRG1-overexpressing BMSCs on the repair of SCI, and investigated the possible underlying mechanisms.

Materials And Methods

Animals and experimental groups

Adult Sprague-Dawley (SD) rats (4–6 weeks old, 24 males and 24 females) were used for model of SCI. Ten 1-week-old SD rats were used for BMSCs preparation. All rats were obtained from Mudanjiang Medical University Experimental Animal Center, and maintained under specific-pathogen-free conditions at 22 ± 1 °C and 45 ± 5% humidity with ad libitum access to food and water. Animal care and all experimental procedures were performed in accordance with the Guide for the Care and Use of Laboratory Animals published by the US National Institutes of Health (publication no. 85 – 23, revised 1996), and approved by the Animal Care and Use Committee of Mudanjiang Medical University. All efforts were made to minimize the number of animals used and their suffering.

Isolation, culture, and identification of BMSCs

Isolation and culture of BMSCs were performed as previously described [12]. Briefly, ten 1-week-old SD rats were sacrificed by cervical dislocation after ether inhalation. Under sterile conditions, tibias and femurs were collected, and the ends of bones were excised after the adherent soft tissue was removed. Then, the bone marrow was flushed into a culture dish using Dulbecco's modified Eagle's medium (DMEM; Invitrogen, Carlsbad, CA, USA). The fluid was disaggregated by gentle pipetting several times, and filtered through a 200 mesh screen (Thermo Fisher Scientific, Inc., Waltham, MA, USA). After centrifuging, the supernatant was discarded, and cell pellets were resuspended in DMEM supplemented with 10% fetal bovine serum, 1% glutamine and 1% penicillin/streptomycin at a density of 1×10^6 cells/mL. Cells were cultured in plastic dishes at 37 °C in humidified atmosphere under 5% CO_2, and the culture medium was renewed every 3 days. Cell morphology was observed using inverted light microscope (DM2000, Leica Microsystems, Wetzlar, Germany). To identify the cell phenotype, the molecular markers of BMSCs including CD90, CD29 and CD34 (Proteintech, Chicago, IL, USA) were detected by immunofluorescence staining. Cells used in the experiments were after three passages.

NRG1-overexpressing BMSCs generation

The plasmid pcDNA3.1$^{(+)}$-NRG1-IRES/eGFP expressing the GFP-tagged NRG1 gene was synthesized by Cyagen Biosciences Inc. (Guangzhou, China). The BMSCs were seeded into six-well plates and divided into 3 groups: BMSCs, empty-vector BMSCs and NRG1-BMSCs. In the empty-vector BMSCs and NRG1-BMSCs groups, a mixture consisting of 94μL DMEM, 6μL FuGen6 reagent (Roche, Inc. USA) and 3μL empty pcDNA3.1$^{(+)}$ plasmid or pcDNA3.1$^{(+)}$-NRG1 (1 μg/μL) were added respectively. In the BMSCs group, 94μL DMEM and 6μL FuGen6 reagent were added. After 6 h of culture, the medium was replaced with a complete culture medium. To obtain stable transfectants, BMSCs were cultured in selection medium containing G418 (200 μg/mL; Sigma-Aldrich, St. Louis, MO), and the levels of NRG1 were examined by ELISA as described below.

ELISA assay

NRG1 levels in culture medium and cell lysates were measured by using ELISA Kit (USCNLIFE, Wuhan, China) according to the manufacturer's instructions. Briefly, the culture medium supernatant and cell lysates of BMSCs, empty-vector BMSCs and NRG1-BMSCs were collected at 1, 2, 3, 4, 7, 14, 21 and 28 day, and transferred to 96-well plates (Corning, New York, USA). After incubation for 2 h at 37 °C, the plates were then incubated with the biotin-conjugated primary detection antibody followed by the horseradish peroxidase-conjugated secondary antibody for 1 h at 37 °C. After addition of the chromogenic substrate, the plates were incubated for 30 min at 37 °C. The optical density (OD) was detected using an iMark microplate reader (Bio-Rad, Hercules, CA, USA).

Co-culture of BMSCs with oxygen-glucose deprivation PC12 cells

To mimic injured conditions of SCI, PC12 cells (Shanghai Institute of Cell Biology, Chinese Academy of Sciences) subjected to oxygen-glucose deprivation (OGD) were used as an *in vitro* model of SCI. Briefly, PC12 cells were seeded onto the bottom wells of transwell chambers (BD Biosciences, Mississauga, Ontario, Canada) at a density of 5×10^4 cells/well. Cultures were maintained in glucose-free DMEM (Invitrogen, Carlsbad, CA, USA), which were bubbled with N_2 for 5 min prior to use. Then, the transwell chambers were placed into an incubator filled with anaerobic gas mixture (1% O_2, 94% N_2 and 5% CO_2) at 37 °C for 2 h. After OGD treatment, the empty-vector BMSCs and NRG1-BMSCs were seeded respectively onto the upper inserts of transwell chambers (5×10^5 cells/well), and co-cultured with OGD PC12 cells in DMEM supplemented with 10% FBS for 72 h. The PC12 cells maintained in a normoxic condition (5% CO_2 and 95% air) with regular DMEM were as the control cultures.

Neurite outgrowth assay

After co-culture for 72 h, PC12 cells were observed with an inverted phase contrast microscope (Olympus, Tokyo, Japan). Images of three fields per well were taken. Neurite length was measured manually tracing neurite by using Image ProPlus 6.0 imaging software (Media Cybernetics UK, Marlow, UK) and referenced to a known length. Cell processes were defined as neurites when they were longer than the diameter of cell body. A researcher blinded to the experimental protocol counted the number of neuritis for 10 independent cells per field with Image ProPlus 6.0 imaging software as previously studies described [27].

Cell apoptosis analysis

Cell apoptosis was detected with terminal deoxynucleotidyl transferase-mediated deoxyuridine triphosphate nick-end labeling (TUNEL; Roche Boehringer-Mannheim, IN, USA) and Caspase-3 Activity Assay Kit (Beyotime Institute of Biotechnology Haimen, China), respectively. Briefly, PC12 cells were fixed in 4% paraformaldehyde, rinsed in PBS and then incubated for 60 min at 37 °C with TUNEL reaction mixture. The nuclei were counterstained with DAPI (Sigma, Saint Louis, MO, USA). The numbers of total PC12 cells and TUNEL positive cells was counted by an operator blind to the experimental protocol using Image ProPlus 6.0 imaging software. The apoptosis rate was defined as ratio of apoptotic cells to total cells. For assay of Caspase-3 activity, PC12 cells were harvested and rinsed with PBS, and the cells were lysed with lysis buffer. The lysate was collected, centrifuged, and incubated with the mixture composed of 50 μL of cell lysate, 40 μL reaction buffer and 10 μL of 2 mM Caspase-3 substrate (Ac-DEVD-pNA) in 96-well plates at 37 °C for 4 h, the absorbance of p-nitroanilide was measured at 405 nm by using a microplate reader. Caspase-3 activity was defined as a ratio of caspase-3 activation level to control level.

Cell viability assessment

Cell viability was assessed by using Cell Counting Kit-8 (CCK-8, Beyotime Institute of Biotechnology Haimen, China) according to the manufacturer's instructions. Briefly, PC12 cells from each group were seeded in 96-well plates (4×10^4 cells/well) with three replicates, and cultured for 12 h under humid conditions in 5% CO_2 and 95% atmospheric air at 37 °C. After that, 10 μL of CCK-8 solution was added to each culture well and incubated at 37 °C for 4 h. The OD values were measured at 450 nm with a

microplate reader. Cell viability was calculated for the OD value of the ODG, empty-vector BMSCs and NRG1-BMSCs groups as a percent of the OD value of the control group.

Spinal cord hemi-section injury and cell transplantation

Animals were subjected to spinal cord hemi-section injury as described previously [24]. Briefly, rats were anesthetized using 2% pentobarbital (40 mg/kg), and an incision was made at the dorsal midline, followed by cutting the cutaneous tissue and separating the muscle. The laminectomy was performed at the T9 segment. After spinal cord had been exposed, a dorsal hemi-section was conducted using an iridectomy scissors, and removed any residual fibers at the lesion site. The tail was spastically swung and the posterior limb twitching rigidity, confirming that the hemi-section of the spinal cord was completed. Gelatin foam was used to stop bleeding and the muscular and skin was sutured in layers. Rats were divided into: SCI, empty-vector BMSCs, NRG1-BMSCs, and the control (laminectomy only) groups.

On the day of transplantation, empty-vector BMSCs and NRG1-BMSCs were digested with 0.25% trypsin containing 0.02% EDTA to generate cell suspension. At 7 days post-injury, rats in the SCI, empty-vector BMSCs and NRG1-BMSCs groups were re-anesthetized and the injury site was surgically re-exposed. Then, a total of three sites were injected and each site was injected with 3μL DMEM, empty-vector BMSCs or NRG1-BMSCs suspension (1×10^7 cells/mL), respectively. The detailed procedure for the injection was described below, Hamilton syringe was vertically penetrated into the lesion center and 3μL of cell suspension was injected. In addition, 3μL of cell suspension was injected at 1 mm cranial to and caudal to the lesion center and 0.6 mm laterally from midline at a depth of 1.3 mm. Cells were delivered under the control of a microsyringe pump controller (World Precision Instruments, Sarasota, FL, US) at a rate of 0.5 mL/min. To minimize cellular reflux, the needle was left in place for 3 min following the completion of injections.

Locomotion recovery assay

The Basso, Beattie and Bresnahan (BBB) locomotor rating scale [28] was used to evaluate rat motor functions at 0, 7, 14, 21, 28, 35, 42, 49 and 56 days after injury. Briefly, the rats were allowed to walk feely in an open field (80 × 130 × 30 cm) with a pasteboard-covered nonslippery floor. In each testing session, the rats were observed individually for 4 min by two trained observers. The hindlimb locomotion was scored from 0 (complete paralysis) to 21 points (normal locomotion). The means of scores were used for analysis. The inclined plane test was performed at 0, 7, 14, 21, 28, 35, 42, 49 and 56 days as the method described previously[29]. In brief, rats were placed with their body axis perpendicular to an orientation of the plate covered with a rubber mat containing horizontal ridges spaced 3 mm apart, and evaluate the maximum vertical axis of the inclined plate. The maximum angle at which a rat maintained its position for 5 sec without falling was recorded for analysis. Footprint analysis was carried out as previously described [30]. In short, the animal's forepaws and hindpaws were brushed with red and blue nontoxic dye, respectively, and the rats were required to walk across a paper lined runway (3 feet long, 3 inches wide) to obtain an edible treat in a darkened box at the end, and the footprints were scanned for analysis.

Histological examination

At 56 days after SCI, rats from each group were anesthetized with 10% chloral hydrate (3.0 mL/kg, i.p.), transcardially perfused with heparinized saline, and followed with 4% paraformaldehyde. The spinal cord segments around the injured site (2.0 cm) were collected, fixed in 4% paraformaldehyde overnight, and then embedded in paraffin, followed by preparation of transverse sections (5 μm). The sections were incubated in 0.1% Cresyl violet Nissl staining solution (Sigma-Aldrich, St. Louis, MO, USA) according to the manufacturer's instructions. Neuronal chromatolysis (defined as dispersion or loss of Nissl bodies) was detected, and the chromatolytic proportions (neurons versus total neurons) were calculated. The integrated optical density (OD) of Nissl bodies were measured using Image Pro Plus 6.0 imaging software by an observer blind to the groups, as previous study described [31].

Immunofluorescence analysis

The immunofluorescence staining was performed as previously described [32]. Briefly, the spinal cord segments were collected, fixed in 4% paraformaldehyde, and then serial 10 μm transverse sections were cut using a cryostat microtome (Leica, Nussloch, Germany). The sections of the injury epicenter were selected and incubated with a blocking buffer (1% bovine serum albumin diluted in 0.1% PBS, with Triton X-100) for 2 h at 4 °C. The sections were incubated with growth-associated protein 43 (GAP43; 1:400, Cell signaling technology, Danvers, MA, USA) at 4 °C overnight. On the next day, the sections were incubated with the secondary antibody for 2 h at 37 °C. Cell nuclei were counterstained with DAPI solution. The sections were photographed using a fluorescence microscope (Olympus BX51TR, Olympus Corp., Tokyo, Japan), and the camera parameters were kept constant during imaging. For quantitative analysis of the GAP43 expression, integral fluorescence density was measured with Image-Pro Plus 6.0 software by an operator blind to the groups, as previous study described [33].

Western blot analysis

At 56 days after SCI, the spinal cord segments around the injured site were collected, and homogenized in RIPA buffer (Beyotime Institute of Biotechnology Haimen, China) with 1% Phenylmethylsulfonyl fluoride and protease inhibitor at 4 °C. After centrifugation at 12,000 rpm for 10 min, the supernatant was collected and quantified by BCA Protein Assay Kit. An equal amount of total protein (30 mg) was loaded and separated by sodium dodecyl sulfate polyacrylamide gel and transferred onto polyvinylidenefluoride (PVDF) membranes (Millipore, Billerica, MA, USA). The membranes were blocked with 5% non-fat milk in TBS-T (10 mmol/L Tris, 150 mmol/L NaCl and 0.1% Tween 20, pH 7.5) for 2 h at 37 °C, and then the membranes were incubated at overnight with GAP43 (1:1000), Cleaved-caspase-3, Bcl2, Bax (1:1000; proteintech, Chicago, IL, USA) and β-actin (1:2000; Cell Signaling Technology). On the following day, the membranes were washed in TBS-T and incubated with the appropriate secondary antibodies for 2 h at 37 °C. The target protein bands were visualized using chemiluminescence luminol reagents (Millipore, Billerica, MA, USA). Blots were imaged by Molecular Image®ChemiDocTM XRS^{+} with Image LabTM Software (Bio-Rad, Hercules, CA, USA). Quantitative data were obtained by Image J 1.50b Gel Analyzer

(National Institutes of Health, Washington, DC, USA). Western blot data were normalized relative to the density of the β-actin bands.

Statistical analysis

All data were presented as mean ± S.E.M. A multifactorial analysis of variance (ANOVA) for repeated measurement was employed for analyzing BBB scores and maximum angles of the inclined plane test. One-way ANOVA was employed for analyzing other data followed by LSD (equal variances assumed) or Dunnett's T3 (equal variances not assumed) post hoc test with SPSS 17.0 software package. Statistical significance was set at $P < 0.05$.

Results

BMSCs primary culture and identification

At 48 h after seeding, the cells displayed a globular shape, had good refraction, and evenly scattered. At 72 h, a large number of attached, round cells were observed, and accompanied by some irregular or triangular cells with tiny processes. Cell proliferation was slow during the first 3–4 days, and accelerated on 5–10 days to form distinct colonies, and majority of cells presented with long-fusiform shape with lucent cytoplasm (Fig. 1a). By the third passage, cells were relatively uniform in appearance, and developed into short or long spindle-shaped (Fig. 1b). The immunofluorescence staining showed that cells were positive for BMSCs markers CD90 and CD29 (Fig. 1c-h), while they were negative for the hematopoietic cell surface marker CD34 (Fig. 1i-k).

Transfection and overexpression of the NRG1 gene in BMSCs

After the pcDNA3.1$^{(+)}$-NRG1-IRES/eGFP plasmid (Fig. 2a) was transfected into BMSCs, weak green fluorescence was initially observed only at some cells under fluorescence microscope. After 48 h, over 80% of BMSCs displayed bright green fluorescence (Fig. 2b-d). To measure the level of NRG1 in BMSCs, ELISA was performed. As shown in Fig. 2e and f, the level of NRG1 was slightly high in culture supernatant of NRG1-BMSCs group, and statistical significance was observed beginning at the 72 h after transfection compared with the BMSCs and empty-vector BMSCs groups ($P < 0.05$), and the high levels of NRG1 continued for weeks. Likewise, NRG1 level in cell lysate of NRG1-BMSCs presented a similar increasing trend as that in the culture supernatants (Fig. 2g, h).

Effects of NRG1-BMSCs on neurite outgrowth in PC12 cells after ODG injury

To evaluate the effects of NRG1-BMSCs on neurite outgrowth after OGD insult, the length and number of neurites in PC12 cells were initially assessed. As shown in Fig. 3a-f, a abundant of long neurites were

observed in PC12 cells in the control group. By contrast, the length and number of neurites in PC12 cells were notably reduced following OGD insult compared to the control group ($P < 0.05$). After co-cultured with NRG1-BMSCs, the length and number of neurites were markedly increased ($P < 0.05$), even though it was not restored to the level of the control group ($P < 0.05$). In addition, the length and number of neurites trended to increase in the empty-vector BMSCs group, however, the difference was not statistically significant compared with the OGD group ($P > 0.05$).

To further test the effects of NRG1-BMSCs on neurite growth, GAP43, a marker of neurite growth, in PC12 cells we analyzed. As shown in Fig. 3g, the level of GAP43 was significantly decreased in the ODG group as compared with that in the control group ($P < 0.05$); however, the decrease in GAP43 induced by ODG was increased following co-cultured with NRG1-BMSCs ($P < 0.05$), even though it was not restored to the level of the control group ($P < 0.05$). Moreover, the GAP43 level trended to increase in the empty-vector BMSCs group, whereas the difference was not statistically significant as compared with that in the OGD group ($P > 0.05$). These results indicated that NRG1-BMSCs could promote neurite outgrowth in PC12 cells after ODG insult.

Effects of NRG1-BMSCs on cell apoptosis and viability after ODG injury

To confirm whether NRG1-BMSCs could rescue PC12 cells from ODG-induced apoptosis, TUNEL assay staining was initially performed (Fig. 4a). As shown in Fig. 4b, the apoptosis rate was significantly increased in the ODG group compared with that in the control group ($P < 0.05$). After co-cultured with NRG1-BMSCs, the apoptosis rate was notably decreased relative to the ODG group ($P < 0.05$), even though it was not restored to the level of the control group ($P < 0.05$). The proportion of apoptotic cells was slightly decreased in the empty-vector BMSCs group, however the apoptotic proportion did not vary significantly compared with that in the ODG group ($P > 0.05$). Next, the anti-apoptotic effects of NRG1-BMSCs were confirmed based on colorimetric assay of Caspase-3 activity. As shown in Fig. 4c, in contrast to the control group, Caspase-3 activity was increased in the ODG group ($P < 0.05$); following co-cultured with NRG1-BMSCs, however, Caspase-3 activity was reduced relative to the ODG group ($P < 0.05$), even though it was not restored to the level of the control group ($P < 0.05$). Additionally, there was no significant difference in Caspase-3 activity between the empty-vector BMSCs and ODG groups ($P > 0.05$). Then, the effects of NRG1-BMSCs on cell viability was assessed. As illustrated in Fig. 4d, the viability of PC12 cells was markedly reduced in the OGD group as compared with that in the control group ($P < 0.05$). Compared with the ODG group, cell viability was elevated after co-cultured with NRG1-BMSCs ($P < 0.05$), even though it was not restored to the level of the control group ($P < 0.05$). Although the viability of PC12 cells tended to increase in the empty-vector BMSCs group, the difference was not statistically significant compared to the OGD group ($P > 0.05$). These results indicated that NRG1-BMSCs could inhibit PC12 cell apoptosis and enhance cell viability after ODG insult.

Effects of NRG1-BMSCs on functional recovery after SCI

To identify the effects of NRG1-BMSCs on motor recovery after SCI, the BBB rating scale, inclined plane test and footprint recording were performed. As shown in Fig. 5a, the BBB scores of rats in the SCI, empty-vector BMSCs and NRG1-BMSCs groups were similar during first 3 days after injury. Within 3–20 days, although the BBB scores of NRG1-BMSCs group were slightly higher than those in the SCI group, it did not reach the level of statistical significance ($P > 0.05$). From the 21th day after cell transplantation, BBB scores of the NRG1-BMSCs group were notably higher than those in the SCI group ($P < 0.05$), even though it was not restored to the level of control group ($P < 0.05$). In addition, BBB scores of the empty-vector BMSCs group tended to increase, however the difference was not statistically significant relative to the SCI group ($P > 0.05$). Consistent with these findings, the angles of inclined-plane test were higher in the NRG1-BMSCs group compared with those in the SCI group ($P < 0.05$), even though it was not restored to the level of the control group ($P < 0.05$) (Fig. 5b). Although the inclined-plane angles tended to increase in the empty-vector BMSCs group, the difference was not statistically significant as compared to the SCI group ($P > 0.05$). As shown in Fig. 5c, footprint assay showed that rats from the NRG1-BMSCs group displayed consistent forelimb-hindlimb coordination and very little toe dragging after 21 days administration of NRG1-BMSCs. By contrast, rat footprints obtained from the SCI and empty-vector BMSCs groups displayed inconsistent coordination and extensive drags as revealed by ink streaks. These results indicated that NRG1-BMSCs could accelerate motor functional recovery after SCI.

Effects of NRG1-BMSCs on neuronal damage after SCI

To test whether engrafted NRG1-BMSCs could attenuate neuronal damage after SCI, Nissl staining was performed. In the control group, neurons were deeply stained with granular-like morphology, and few chromatolytic neurons were observed (Fig. 6a, b). By contrast, in the SCI group, large numbers of neurons were dimly stained with chromatolytic appearance (Fig. 6c, d). Similarly, most neurons in the empty-vector BMSCs group displayed chromatolytic changes (Fig. 6e, f). After transplantation of NRG1-BMSCs, the loss of Nissl bodies was improved, and less chromatolytic neurons were observed in the NRG1-BMSCs group (Fig. 6g, h). As illustrated in Fig. 6i, the chromatolytic proportions were higher in the SCI group than that in the control group ($P < 0.05$). After NRG1-BMSCs administration, however, the proportions were decreased in NRG1-BMSCs group compared with that in the SCI group ($P < 0.05$), even though it was not restored to the level of control group ($P < 0.05$). In addition, the proportions did not vary significantly between the the empty-vector BMSCs and the SCI groups ($P > 0.05$). Also, we analyzed the optical density of Nissl bodies to further evaluate the neuronal damage. As showed in Fig. 6j, the OD values in SCI group was markedly decreased compared with that in the control group ($P < 0.05$). Compared with the SCI group, the OD values were increased in the NRG1-BMSCs group ($P < 0.05$), even though it was not restored to the level of control group ($P < 0.05$). No significant difference was found in OD values between SCI and empty-vector BMSCs groups ($P > 0.05$). These results suggested that NRG1-BMSCs could attenuate neuronal damage after SCI in rats.

Effects of NRG1-BMSCs on neurite outgrowth after SCI

To determine the effects of NRG1-BMSCs on neurite outgrowth after SCI, the distribution of GAP43 was detected with immunofluorescence staining (Fig. 7a). As shown in Fig. 7b, the fluorescence intensity of GAP43 in the SCI group was significantly decreased compared with that in the control group ($P < 0.05$), whereas the reduced fluorescence intensity due to SCI was increased with NRG1-BMSCs administration ($P < 0.05$), and there was no significant difference in fluorescence intensity between the SCI and empty-vector BMSCs groups ($P > 0.05$). To further test the effect of NRG1-BMSCs on neurite regrowth, GAP43 expression was evaluated by western blot (Fig. 7c). Consistent with fluorescence assay, the level of GAP43 were markedly decreased in the SCI group compared with that in the control group ($P < 0.05$). After administration of NRG1-BMSCs, the level of GAP43 were elevated ($P < 0.05$), even though it was not restored to the level of control group ($P < 0.05$). Moreover, no significant difference was found in GAP43 expression between the SCI and empty-vector BMSCs groups ($P > 0.05$). These results suggested NRG1-BMSCs could facilitate neurite outgrowth after SCI in rats.

Effects of NRG1-BMSCs on cell apoptosis after SCI

To identify whether NRG1-BMSCs could suppress cell apoptosis after SCI, TUNEL staining was performed (Fig. 8a). As shown in Fig. 8b, the apoptosis rate was notably increased in the SCI group compared with that in the control group ($P < 0.05$), however the higher apoptosis rate in the SCI group were reduced following NRG1-BMSCs administration, even though it was not restored to the level of control group ($P < 0.05$). The apoptosis rate tended to decrease in the empty-vector BMSCs group, but it did not vary significantly relative to the SCI group ($P > 0.05$). To further clarify the anti-apoptotic effects of NRG1-BMSCs, the apoptosis-related proteins were also analyzed. As shown in Fig. 8c and e, the levels of cleaved caspase-3 and Bax were significantly increased in the SCI group compared with those in the control group ($P < 0.05$), however the increases of these pro-apoptosis proteins were reversed after NRG1-BMSCs transplantation ($P < 0.05$), even though it was not restored to the level of control group ($P < 0.05$). The levels of cleaved caspase-3 and Bax tended to decrease in the empty-vector BMSCs group, but no significant difference was found between the SCI and empty-vector BMSCs groups ($P > 0.05$). In contrast, the level of Bcl-2 was sharply reduced in the SCI group compared to the control group ($P < 0.05$), whereas the reduction was diminished following NRG1-BMSCs transplantation ($P < 0.05$), even though it was not restored to the level of control group ($P < 0.05$). In addition, the level of Bcl-2 did not vary significantly between the SCI and empty-vector BMSCs groups ($P > 0.05$) (Fig. 8d). These results indicated that NRG1-BMSCs could attenuate cell apoptosis after SCI in rats.

Discussion

In the present study, we evaluated the effects of NRG1-BMSCs on the repair of SCI and explored the possible mechanisms. We found *in vitro* that NRG1-BMSCs could enhance cell viability, expedite neurite growth, and protect PC12 cells from OGD-induced apoptosis. Furthermore, we discovered *in vivo* that NRG1-BMSCs could accelerate rat motor functional recovery, attenuate neuronal damage, facilitate neurite outgrowth, and reduce cell apoptosis. Notably, our data demonstrated that NRG1-BMSCs were also able to regulate apoptosis-related proteins expression after SCI. Our findings collectively suggested

that transplantation of NRG1-BMSCs could accelerate motor functional recovery, which might be, at least partly, through eliciting neurite outgrowth and relieving cell apoptosis after SCI.

SCI is the most difficult traumatic neurological condition to treat in the clinic. Currently, beside surgical intervention, the common approach to treat SCI is applied large doses of steroids, such as methylprednisolone. However, this treatment has been largely discontinued due to its time sensitivity and the severe side effects [34]. A growing body of evidence indicate that BMSCs can ameliorate motor functions in animal models of SCI by regulating diverse pathophysiological events including oxidative stress, apoptosis and inflammatory reactions [35]. It has been widely recognized that axons in mammalian CNS do not regenerate following injury, predominantly due to the inability of neurons to produce neurites for the inhibitory milieu and absence of external growth stimulating or supporting factors [36]. Thus, how to facilitate neurite growth of neurons has become the key therapeutic strategy after SCI.

The NRG1 family is comprised of more than 15 secreted transmembrane proteins, that derived from one of the largest mammalian genes [13]. Numerous studies revealed that NRG1 is a neurotrophic and neuroprotective factor for cortical neurons [37], motor neurons [38], dopaminergic neurons [39] and PC12 cells [40]. As noted previously, NRG1 was also able to protect neurons from ischemia injury [41]. Some researchers discovered that NRG1 acted as an axonal chemoattractant to elicit the axon growth of neurons [42, 43]. Consistent with these findings, we found in this study that NRG1-BMSCs could notably enhance cell viability, facilitate neurite growth, and reduce OGD-induced apoptosis in PC12 cells. There is evidence that GAP43, a protein enriched in growth cones and synaptic terminals, plays a critical role in axonal elongation and synaptogenesis. In line with the notion, we discovered in the present study that NRG1-BMSCs could augment GAP43 expression in PC12 cells following OGD insult. A number of studies revealed that NRG1 involves in neural development [44], and promotes neurons proliferation, migration in the CNS [13]. Interestingly, our data demonstrated in this study that NRG1-BMSCs could facilitate neurite growth in PC12 cells after OGD injury. We speculate that NRG1-BMSCs can effectively promote rat functional recovery, which may be partly associated with the neurotrophic effects of NRG1-BMSCs on facilitating neurite growth after SCI.

Meanwhile, our data demonstrated the neuroprotective effects of NRG1-BMSCs based on the histological changes. Previously, our study revealed that transplantation of Schwann cells (SCs) overexpressing NRG1 could definitely alleviate histological damage after SCI [24]. Moreover, we discovered that co-transplantation of NRG1 overexpressing SCs and BMSCs could reduce spinal cord cystic cavities, and improve motor functional recovery in rats after SCI [45]. In this study, we found that transplantation of NRG1-BMSCs notably reduced neuronal chromatolysis after SCI. Concomitantly, our data also showed that an overt reduction or absence of GAP43 protein expression in SCI rats, which was in agreement with the observations in a previous study [46]. Interestingly, the sharp reduction of GAP43 caused by SCI was distinctly eliminated with NRG1-BMSCs administration. This partly explained by the fact that NRG1-BMSCs might fill the lesion cavities and produce a great of NRG1, as a neurotrophic factor, which improve

the inhospitable microenvironment, thereby reducing neuronal chromatolysis and promoting axonal outgrowth after SCI.

To further investigate the neuroprotective effects and possible mechanisms of NRG1-BMSCs on SCI, we also detected the apoptosis-related proteins expression in spinal cord tissues after SCI. A previous study reported that epidermal growth factor treatment significantly decreased Bax and increased Bcl-2 proteins expression both in spinal cord and frontal cortex, and promoted motor functional recovery and motor neuron survival in rats after SCI [47]. In consistent with these studies, we found in this study that transplantation of NRG1-BMSCs obviously reduced cell apoptosis after SCI in rats. What's more, we found that NRG1-BMSCs administration could effectively enhance Bcl-2 level and decrease Bax expression after SCI. Evidence from multiple sources indicate that Bcl-2 plays a key role in regulation of the apoptotic pathway, and Bax involves in intracellular caspases activation [48, 49]. It is believed that cleaved caspase-3 is a hallmark of programmed cell death, and it performs as a key executor of cell apoptosis [50]. In this study, we discovered that the level of cleaved caspase-3 was markedly elevated in rats after SCI. However, the augment of cleaved caspase-3 induced by SCI were reduced after NRG1-BMSCs administration, which suggested that NRG1-BMSCs participated in regulating apoptotic pathway and preventing cell apoptosis after SCI.

Conclusions

In summary, this study demonstrated that NRG1-overexpressing BMSCs appeared to accelerate rat motor functional recovery after SCI, which might be, at least partly, through facilitating neurite outgrowth and reducing cell apoptosis after SCI. Although the underlying mechanisms remain unclear, our findings suggest that NRG1-BMSCs may be a potential novel approach for the treatment of SCI.

Abbreviations

BMSCs: Bone marrow mesenchymal stem cells; NRG1: Neuregulin1; SCI: Spinal cord injury; OGD: Oxygen-glucose deprivation; CNS: Central nervous system; SD: Sprague-Dawley; DMEM: Dulbecco's modified Eagle's medium; TUNEL: Terminal deoxynucleotidyl transferase-mediated deoxyuridine triphosphate nick-end labeling; CCK-8: Cell Counting Kit-8; BBB: Basso, Beattie and Bresnahan; OD: Optical density; SCs: Schwann cells; GAP43: growth-associated protein 43

Declarations

Acknowledgements

The authors would like to express our gratitude to Prof. Jifei Zhang for her insightful advice on the experimental design.

Authors' contributions

JBY and ZFS designed the experiment and instructed the experiment. GW and HRL collected and analyzed the obtained data. MZ and YW participated in the experimental design and manuscript drafting. YLB conducted cell culture and cell transfection. YL and JFW performed immunofluorescent staining, quantitative Q-PCR and rat model preparation. The authors read and approved the final manuscript.

Funding

This work was supported by the Science Fund Project of Heilongjiang Provincial Health and Family Planning Commission (No. 2019-383), Natural Science Foundation of Heilongjiang, China (LH2020H073), Traditional Chinese Medicine Research Project of Heilongjiang Province (No. ZHY18-167), and Research Fund of Hongqi Hospital affiliated to Mudanjiang Medical University (No. 2018HQ-04).

Availability of data and materials

The datasets used and/or analyzed during the current study are available from the corresponding author on reasonable request.

Ethics approval and consent to participate

Animal care and all experimental protocols were approved by the guidelines of the Institutional Medical Experimental Animal Care Committee of Mudanjiang Medical University.

Consent for publication

Not applicable.

Competing interests

The authors declare that they have no competing interests.

References

1. Karsy M, Hawryluk G. Modern Medical Management of Spinal Cord Injury. Curr Neurol Neurosci Rep. 2019;19:65.
2. Kuzhandaivel A, Nistri A, Mazzone GL, Mladinic M. Molecular Mechanisms Underlying Cell Death in Spinal Networks in Relation to Locomotor Activity After Acute Injury in vitro. Front Cell Neurosci. 2011;5:9.

3. Shao A, Tu S, Lu J, Zhang J. Crosstalk between stem cell and spinal cord injury: pathophysiology and treatment strategies. Stem Cell Res Ther. 2019;10:238.
4. Shroff G. Human Embryonic Stem Cell Therapy in Chronic Spinal Cord Injury: A Retrospective Study. Clin Transl Sci. 2016;9:168–75.
5. Tashiro S, Nishimura S, Iwai H, Sugai K, Zhang L, Shinozaki M, Iwanami A, Toyama Y, Liu M, Okano H, et al. Functional Recovery from Neural Stem/Progenitor Cell Transplantation Combined with Treadmill Training in Mice with Chronic Spinal Cord Injury. Sci Rep. 2016;6:30898.
6. Khankan RR, Griffis KG, Haggerty-Skeans JR, Zhong H, Roy RR, Edgerton VR, Phelps PE. Olfactory Ensheathing Cell Transplantation after a Complete Spinal Cord Transection Mediates Neuroprotective and Immunomodulatory Mechanisms to Facilitate Regeneration. J Neurosci. 2016;36:6269–86.
7. Xie XM, Shi LL, Shen L, Wang R, Qi Q, Wang QY, Zhang LJ, Lu HZ, Hu JG. Co-transplantation of MRF-overexpressing oligodendrocyte precursor cells and Schwann cells promotes recovery in rat after spinal cord injury. Neurobiol Dis. 2016;94:196–204.
8. Neirinckx V, Agirman G, Coste C, Marquet A, Dion V, Rogister B, Franzen R, Wislet S. Adult bone marrow mesenchymal and neural crest stem cells are chemoattractive and accelerate motor recovery in a mouse model of spinal cord injury. Stem Cell Res Ther. 2015;6:211.
9. Hoch AI, Leach JK. Concise review: optimizing expansion of bone marrow mesenchymal stem/stromal cells for clinical applications. Stem Cells Transl Med. 2015;4:412.
10. Wright KT, El Masri W, Osman A, Chowdhury J, Johnson WE. Concise review: Bone marrow for the treatment of spinal cord injury: mechanisms and clinical applications. Stem Cells. 2011;29:169–78.
11. Calio ML, Marinho DS, Ko GM, Ribeiro RR, Carbonel AF, Oyama LM, Ormanji M, Guirao TP, Calio PL, Reis LA, et al. Transplantation of bone marrow mesenchymal stem cells decreases oxidative stress, apoptosis, and hippocampal damage in brain of a spontaneous stroke model. Free Radic Biol Med. 2014;70:141–54.
12. Feng N, Hao G, Yang F, Qu F, Zheng H, Liang S, Jin Y. Transplantation of mesenchymal stem cells promotes the functional recovery of the central nervous system following cerebral ischemia by inhibiting myelin-associated inhibitor expression and neural apoptosis. Exp Ther Med. 2016;11:1595–600.
13. Falls DL. Neuregulins: functions, forms, and signaling strategies. Exp Cell Res. 2003;284:14–30.
14. Garratt AN, Britsch S, Birchmeier C. Neuregulin, a factor with many functions in the life of a schwann cell. Bioessays. 2000;22:987–96.
15. Buonanno A, Fischbach GD. Neuregulin and ErbB receptor signaling pathways in the nervous system. Curr Opin Neurobiol. 2001;11:287–96.
16. Newbern J, Birchmeier C. Nrg1/ErbB signaling networks in Schwann cell development and myelination. Semin Cell Dev Biol. 2010;21:922–8.
17. Odiete O, Hill MF, Sawyer DB. Neuregulin in cardiovascular development and disease. Circ Res. 2012;111:1376–85.

18. Ortega MC, Bribian A, Peregrin S, Gil MT, Marin O, de Castro F. Neuregulin-1/ErbB4 signaling controls the migration of oligodendrocyte precursor cells during development. Exp Neurol. 2012;235:610–20.
19. Mei L, Xiong WC. Neuregulin 1 in neural development, synaptic plasticity and schizophrenia. Nat Rev Neurosci. 2008;9:437–52.
20. Brinkmann BG, Agarwal A, Sereda MW, Garratt AN, Muller T, Wende H, Stassart RM, Nawaz S, Humml C, Velanac V, et al. Neuregulin-1/ErbB signaling serves distinct functions in myelination of the peripheral and central nervous system. Neuron. 2008;59:581–95.
21. Birchmeier C, Bennett DL. Neuregulin/ErbB Signaling in Developmental Myelin Formation and Nerve Repair. Curr Top Dev Biol. 2016;116:45–64.
22. Li Y, Lein PJ, Ford GD, Liu C, Stovall KC, White TE, Bruun DA, Tewolde T, Gates AS, Distel TJ, et al. Neuregulin-1 inhibits neuroinflammatory responses in a rat model of organophosphate-nerve agent-induced delayed neuronal injury. J Neuroinflammation. 2015;12:64.
23. Li Y, Xu Z, Ford GD, Croslan DR, Cairobe T, Li Z, Ford BD. Neuroprotection by neuregulin-1 in a rat model of permanent focal cerebral ischemia. Brain Res. 2007;1184:277–83.
24. Zhang J, Zhao F, Wu G, Li Y, Jin X. Functional and histological improvement of the injured spinal cord following transplantation of Schwann cells transfected with NRG1 gene. Anat Rec (Hoboken). 2010;293:1933–46.
25. Lok J, Zhao S, Leung W, Seo JH, Navaratna D, Wang X, Whalen MJ, Lo EH. Neuregulin-1 effects on endothelial and blood-brain-barrier permeability after experimental injury. Transl Stroke Res. 2012;3(Suppl 1):119–24.
26. Lok J, Sardi SP, Guo S, Besancon E, Ha DM, Rosell A, Kim WJ, Corfas G, Lo EH. Neuregulin-1 signaling in brain endothelial cells. J Cereb Blood Flow Metab. 2009;29:39–43.
27. Kubota K, Fukue H, Sato H, Hashimoto K, Fujikane A, Moriyama H, Watanabe T, Katsurabayashi S, Kainuma M, Iwasaki K. The Traditional Japanese Herbal Medicine Hachimijiogan Elicits Neurite Outgrowth Effects in PC12 Cells and Improves Cognitive in AD Model Rats via Phosphorylation of CREB. Front Pharmacol. 2017;8:850.
28. Basso DM, Beattie MS, Bresnahan JC. A sensitive and reliable locomotor rating scale for open field testing in rats. J Neurotrauma. 1995;12:1–21.
29. Rivlin AS, Tator CH. Objective clinical assessment of motor function after experimental spinal cord injury in the rat. J Neurosurg. 1977;47:577–81.
30. Faulkner JR, Herrmann JE, Woo MJ, Tansey KE, Doan NB, Sofroniew MV. Reactive astrocytes protect tissue and preserve function after spinal cord injury. J Neurosci. 2004;24:2143–55.
31. Yan X, Lei F, Hu Y, Nie L, Jia Q, Zhou H, Zhao F, Zheng Y. Hydrogen sulfide protects neonatal rat medulla oblongata against prenatal cigarette smoke exposure via anti-oxidative and anti-inflammatory effects. Environ Toxicol Pharmacol. 2018;57:151–8.
32. Bai L, Mei X, Shen Z, Bi Y, Yuan Y, Guo Z, Wang H, Zhao H, Zhou Z, Wang C, et al. Netrin-1 Improves Functional Recovery through Autophagy Regulation by Activating the AMPK/mTOR Signaling Pathway in Rats with Spinal Cord Injury. Sci Rep. 2017;7:42288.

33. Zhao F, Lei F, Yan X, Zhang S, Wang W, Zheng Y. Protective Effects of Hydrogen Sulfide Against Cigarette Smoke Exposure-Induced Placental Oxidative Damage by Alleviating Redox Imbalance via Nrf2 Pathway in Rats. Cell Physiol Biochem. 2018;48:1815–28.
34. Cheng Z, Bosco DB, Sun L, Chen X, Xu Y, Tai W, Didier R, Li J, Fan J, He X, Ren Y. Neural Stem Cell-Conditioned Medium Suppresses Inflammation and Promotes Spinal Cord Injury Recovery. Cell Transplant. 2017;26:469–82.
35. Gu C, Li H, Wang C, Song X, Ding Y, Zheng M, Liu W, Chen Y, Zhang X, Wang L. Bone marrow mesenchymal stem cells decrease CHOP expression and neuronal apoptosis after spinal cord injury. Neurosci Lett. 2017;636:282–9.
36. Mohit AA. Cellular Events and Pathophysiology of SCI. Spine (Phila Pa 1976). 2016;41(Suppl 7):28.
37. Agarwal A, Zhang M, Trembak-Duff I, Unterbarnscheidt T, Radyushkin K, Dibaj P, Martins de Souza D, Boretius S, Brzozka MM, Steffens H, et al. Dysregulated expression of neuregulin-1 by cortical pyramidal neurons disrupts synaptic plasticity. Cell Rep. 2014;8:1130–45.
38. Ricart K, Pearson J, Viera RJ, Cassina L, Kamaid P, Carroll A, Estevez SL. AG. Interactions between beta-neuregulin and neurotrophins in motor neuron apoptosis. J Neurochem. 2006;97:222–33.
39. Depboylu C, Rosler TW, de Andrade A, Oertel WH, Hoglinger GU. Systemically administered neuregulin-1beta1 rescues nigral dopaminergic neurons via the ErbB4 receptor tyrosine kinase in MPTP mouse models of Parkinson's disease. J Neurochem. 2015;133:590–7.
40. Di Segni A, Shaharabani E, Stein R, Pinkas-Kramarski R. Neuregulins rescue PC12-ErbB-4 cells from cell death induced by beta-amyloid peptide: involvement of PI3K and PKC. J Mol Neurosci. 2005;26:57–69.
41. Croslan DR, Schoell MC, Ford GD, Pulliam JV, Gates A, Clement CM, Harris AE, Ford BD. Neuroprotective effects of neuregulin-1 on B35 neuronal cells following ischemia. Brain Res. 2008;1210:39–47.
42. Gerecke KM, Wyss JM, Carroll SL. Neuregulin-1beta induces neurite extension and arborization in cultured hippocampal neurons. Mol Cell Neurosci. 2004;27:379–93.
43. Lopez-Bendito G, Cautinat A, Sanchez JA, Bielle F, Flames N, Garratt AN, Talmage DA, Role LW, Charnay P, Marin O, et al. Tangential neuronal migration controls axon guidance: a role for neuregulin-1 in thalamocortical axon navigation. Cell. 2006;125:127–42.
44. Lee KF, Simon H, Chen H, Bates B, Hung MC, Hauser C. Requirement for neuregulin receptor erbB2 in neural and cardiac development. Nature. 1995;378:394–8.
45. Zhang JF, Zhao FS, Wu G, Kong QF, Sun B, Cao J, Zhang Y, Wang JH, Zhang J, Jin XD, et al. Therapeutic effect of co-transplantation of neuregulin-1-transfected Schwann cells and bone marrow stromal cells on spinal cord hemisection syndrome. Neurosci Lett. 2011;497:128–33.
46. Khan IU, Yoon Y, Kim A, Jo KR, Choi KU, Jung T, Kim N, Son Y, Kim WH, Kweon OK. Improved Healing after the Co-Transplantation of HO-1 and BDNF Overexpressed Mesenchymal Stem Cells in the Subacute Spinal Cord Injury of Dogs. Cell Transplant. 2018;27:1140–53.

47. Ozturk AM, Sozbilen MC, Sevgili E, Dagci T, Ozyalcin H, Armagan G. Epidermal growth factor regulates apoptosis and oxidative stress in a rat model of spinal cord injury. Injury. 2018;49:1038–45.
48. Ouyang YB, Giffard RG. MicroRNAs affect BCL-2 family proteins in the setting of cerebral ischemia. Neurochem Int. 2014;77:2–8.
49. Ma SB, Nguyen TN, Tan I, Ninnis R, Iyer S, Stroud DA, Menard M, Kluck RM, Ryan MT, Dewson G. Bax targets mitochondria by distinct mechanisms before or during apoptotic cell death: a requirement for VDAC2 or Bak for efficient Bax apoptotic function. Cell Death Differ. 2014;21:1925–35.
50. D'Amelio M, Sheng M, Cecconi F. Caspase-3 in the central nervous system: beyond apoptosis. Trends Neurosci. 2012;35:700–9.

Figures

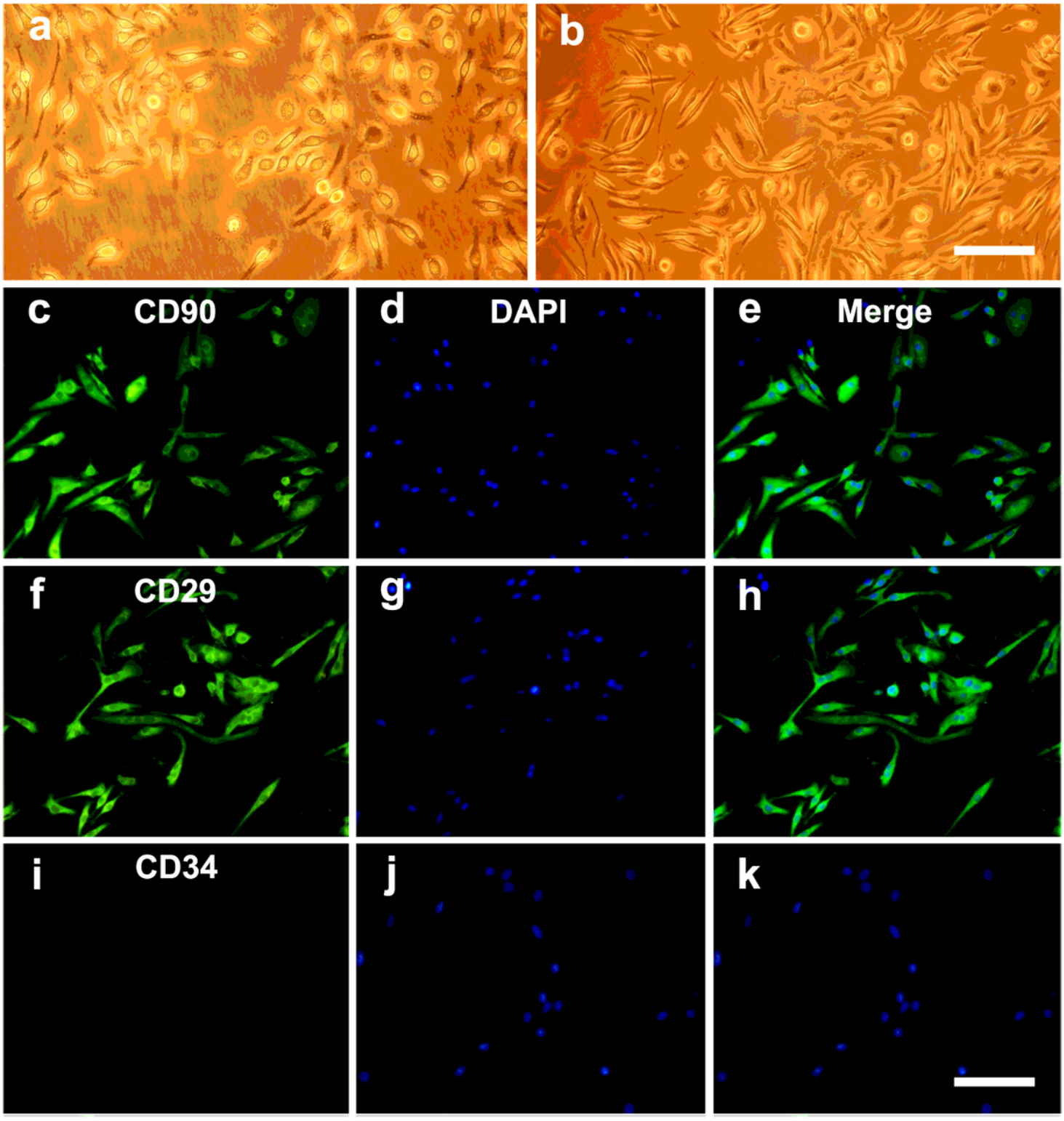

Figure 1

BMSCs culture and identification. a The BMSCs culture on day 7. b The BMSCs culture at the third passage. c-k Immunofluorescent identification of BMSCs with CD90, CD29 and CD34. Scale bars: 100μm in a-k.

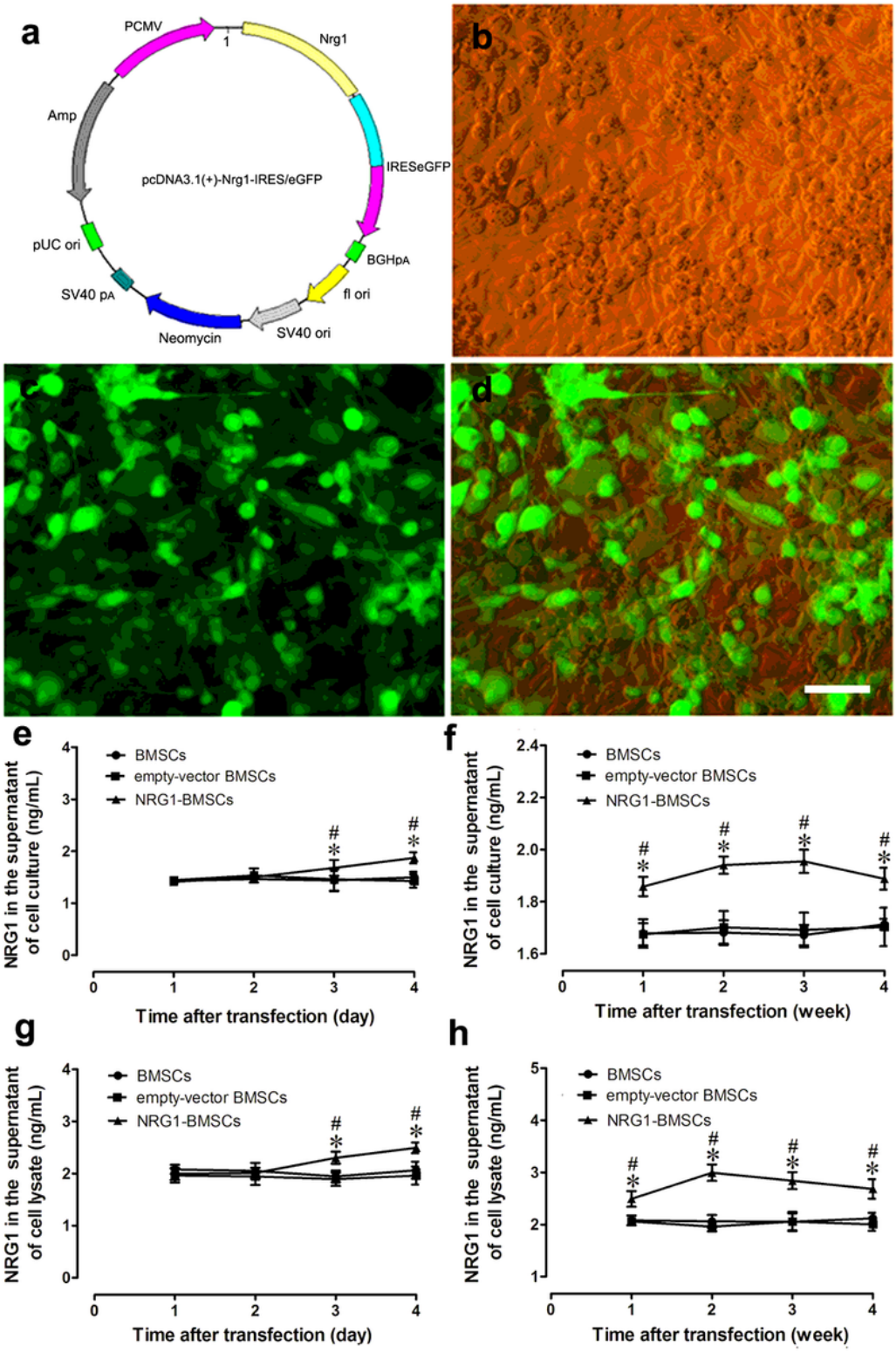

Figure 2

The map of pcDNA3.1(+)-NRG1-IRES/eGFP plasmid and NRG1 expression after transfection. a Plasmid map of pcDNA3.1(+)-NRG1-IRES/eGFP. b Optical microscopy image of NRG1-BMSCs. c Fluorescence image of NRG1-BMSCs. d Overlap of fluorescence and optical microscopy image of NRG1-BMSCs. e-h NRG1 levels in culture supernatant and lysate of BMSCs, empty-vector and NRG1-BMSCs, respectively, at

different time points. Scale bar: 100μm. *P<0.05 vs. BMSCs group; #P<0.05 vs. empty-vector BMSCs group.

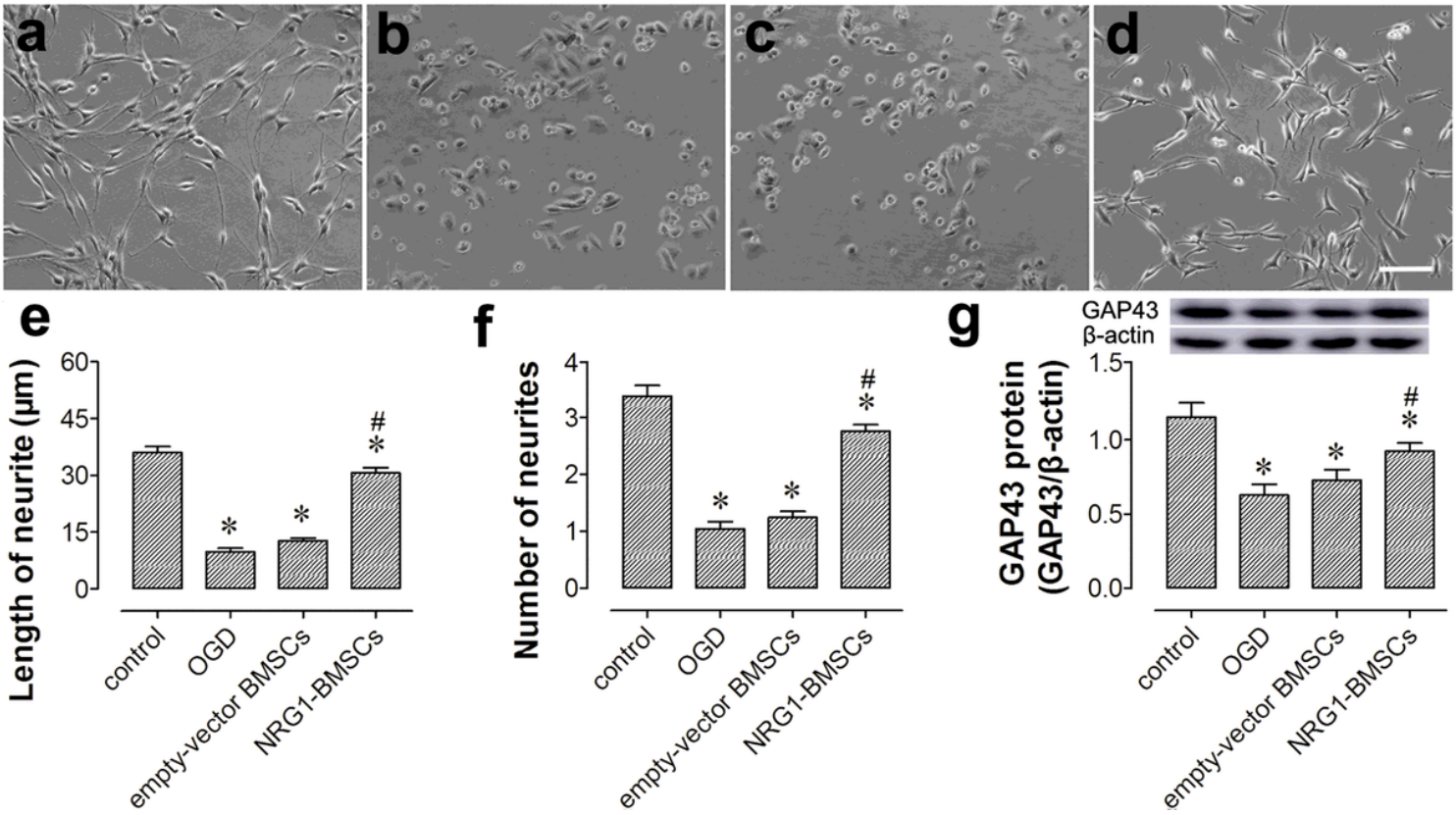

Figure 3

Effects of NRG1-BMSCs on neurite outgrowth in PC12 cells after OGD injury. a-d Images of PC12 cells of the control, OGD, empty-vector BMSCs and NRG1-BMSCs groups, respectively; e-f Comparisons of the length and number of neurites in PC12 cells of the control, OGD, empty-vector BMSCs and NRG1-BMSCs groups. g Representative immunoblots (upper) and densitometric analysis (lower) of GAP43 in the control, OGD, empty-vector BMSCs and NRG1-BMSCs groups. Scale bar: 100μm. *P<0.05 vs. control group; #P<0.05 vs. OGD group.

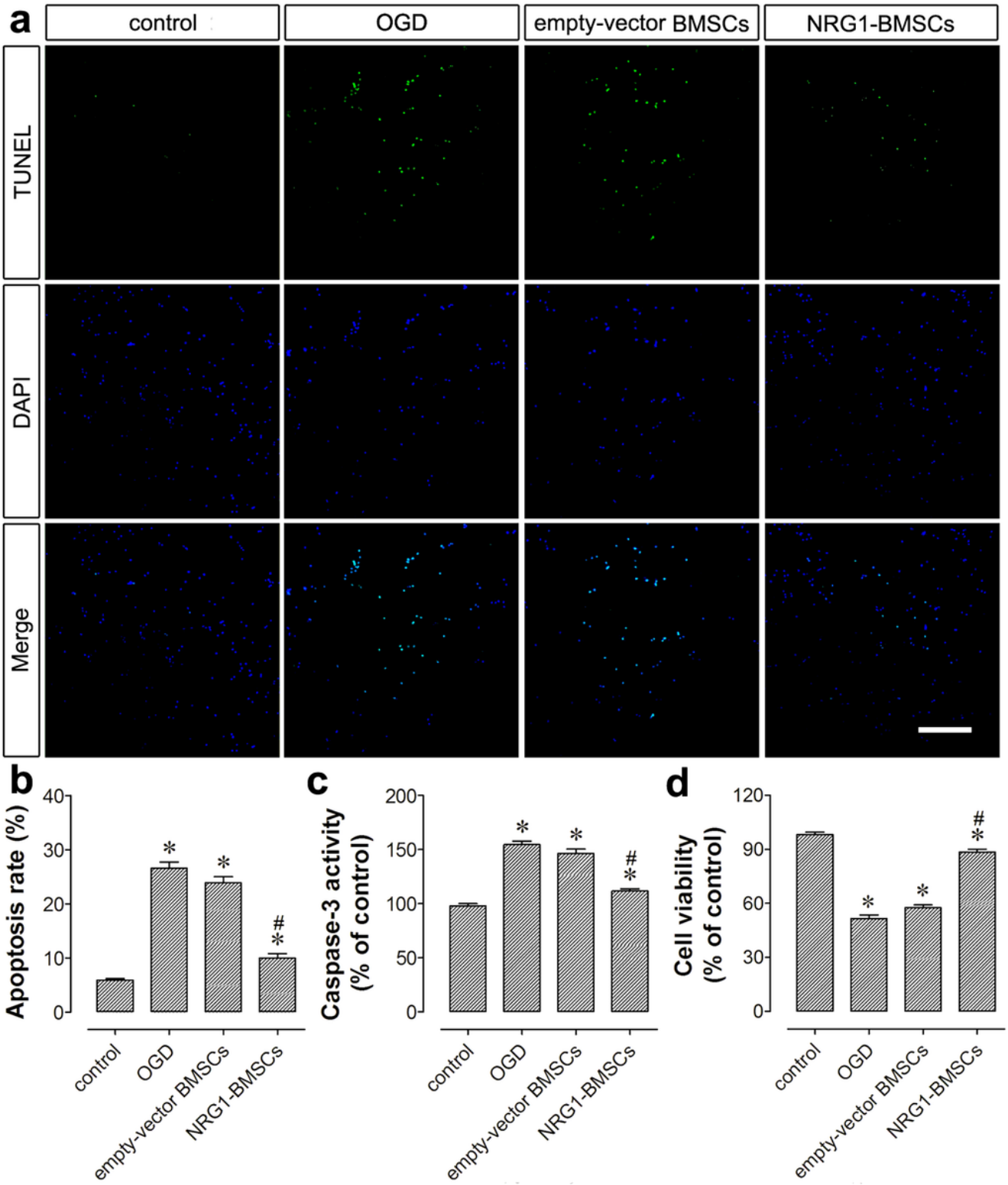

Figure 4

Effects of NRG1-BMSCs on cell apoptosis and viability in PC12 cells after OGD injury. a Images of PC12 cells stained with TUNEL (green) and DAPI (blue). b-c Comparisons of the apoptosis rate, Caspase-3 activity and cell viability of PC12 cells in control, OGD, empty-vector BMSCs and NRG1-BMSCs groups, respectively. Scale bar: 100μm. *P<0.05 vs. control group; #P<0.05 vs. ODG group.

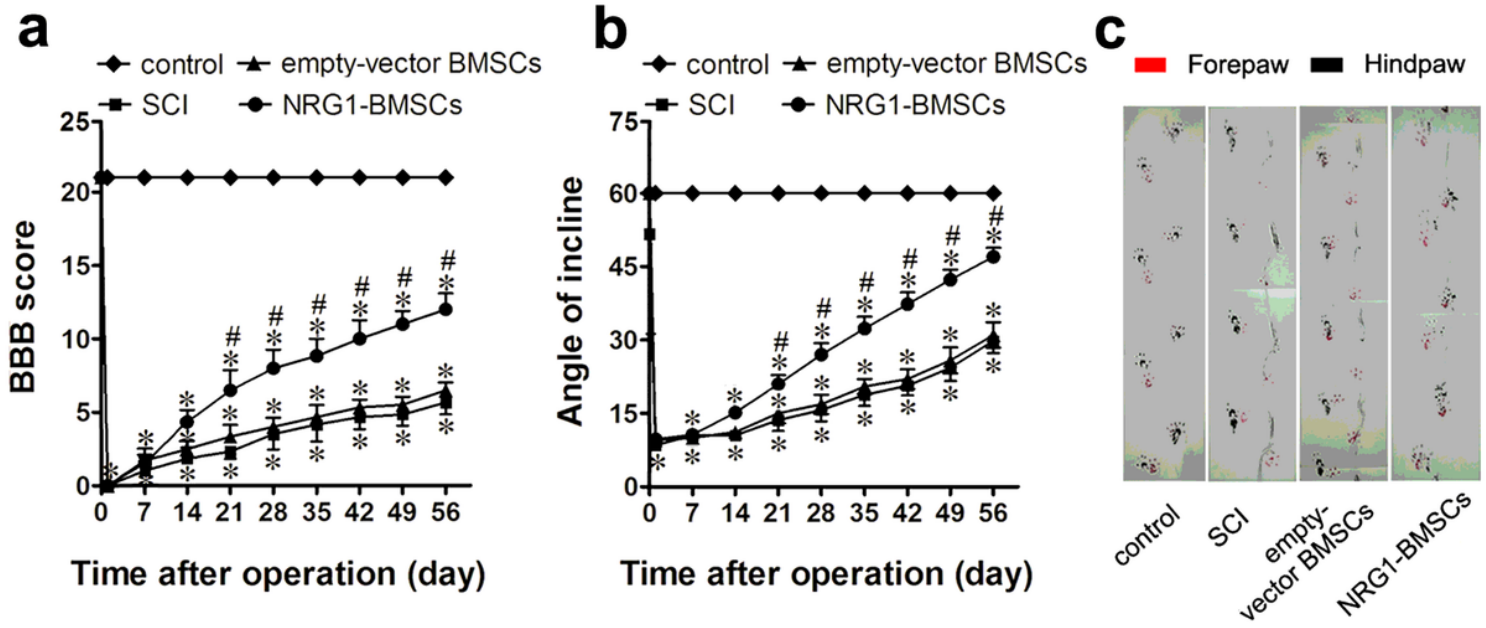

Figure 5

Effects of NRG1-BMSCs transplantation on motor functional recovery after SCI. a-b The BBB score and angle of inclined-plane of the control, SCI, empty-vector BMSCs and NRG1-BMSCs groups. c Rat footprints of the control, SCI, empty-vector BMSCs and NRG1-BMSCs groups at 56 days after injury. *P<0.05 vs. control group; #P<0.05 vs. SCI group.

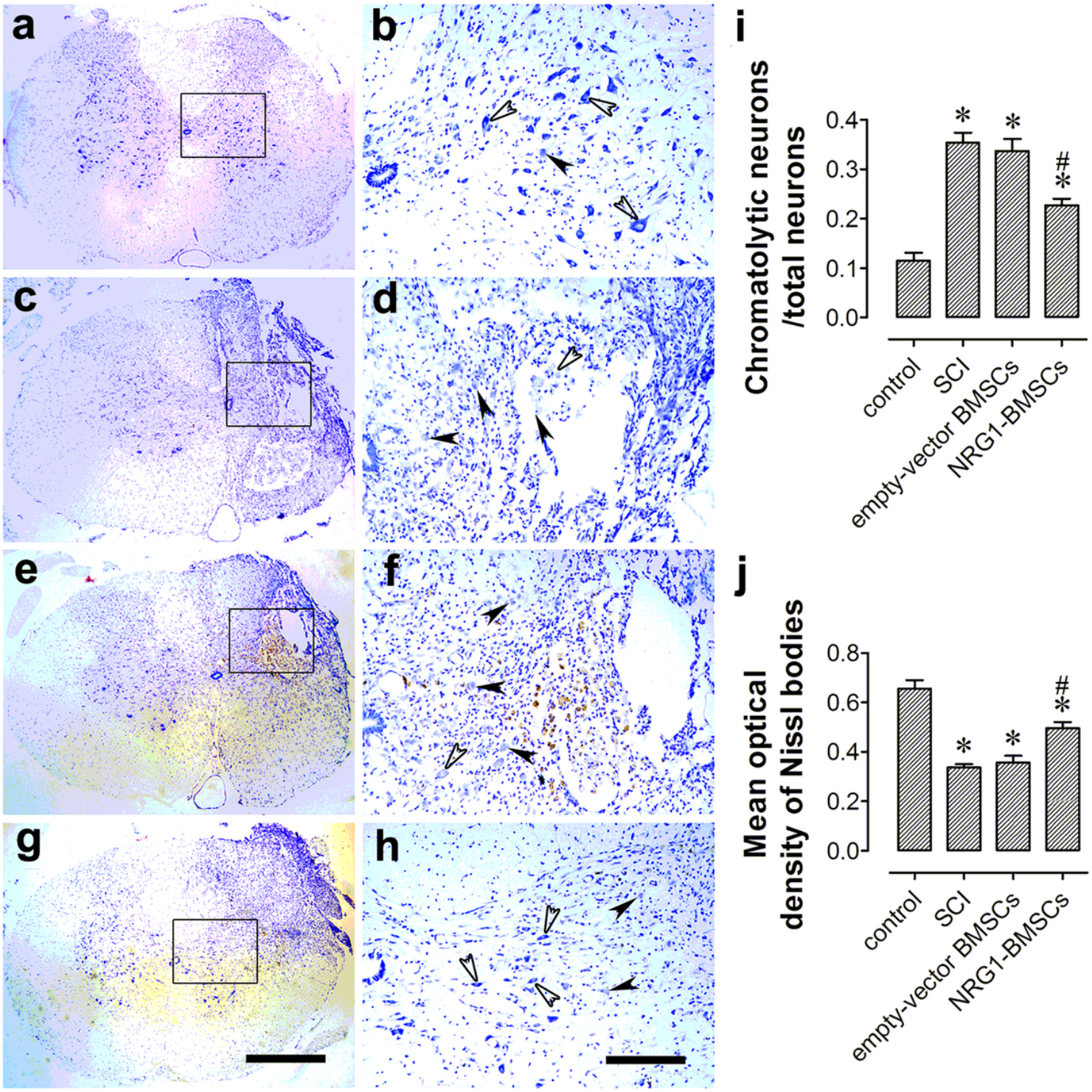

Figure 6

Effects of NRG1-BMSCs on neuronal damage after SCI. a, c, e, g Nissl staining of transverse sections of spinal cords from the control, SCI, empty-vector BMSCs and NRG1-BMSCs groups, respectively, at 56 days after injury; b, d, f, h Higher magnification images of the sites indicated by the black squares in a, c, e, g, respectively. The normal and chromatolytic neurons were labeled respectively with blank arrowheads and black arrowheads. Scale bars: 2mm in a, c, e, g; 100μm in b, d, f, h. i Proportions of chromatolytic neurons to total neurons in the control, SCI, empty-vector BMSCs and NRG1-BMSCs groups. j Comparison

of optical density (OD) of Nissl bodies in the control, SCI, empty-vector BMSCs and NRG1-BMSCs groups. *P<0.05 vs. control group; #P<0.05 vs. SCI group.

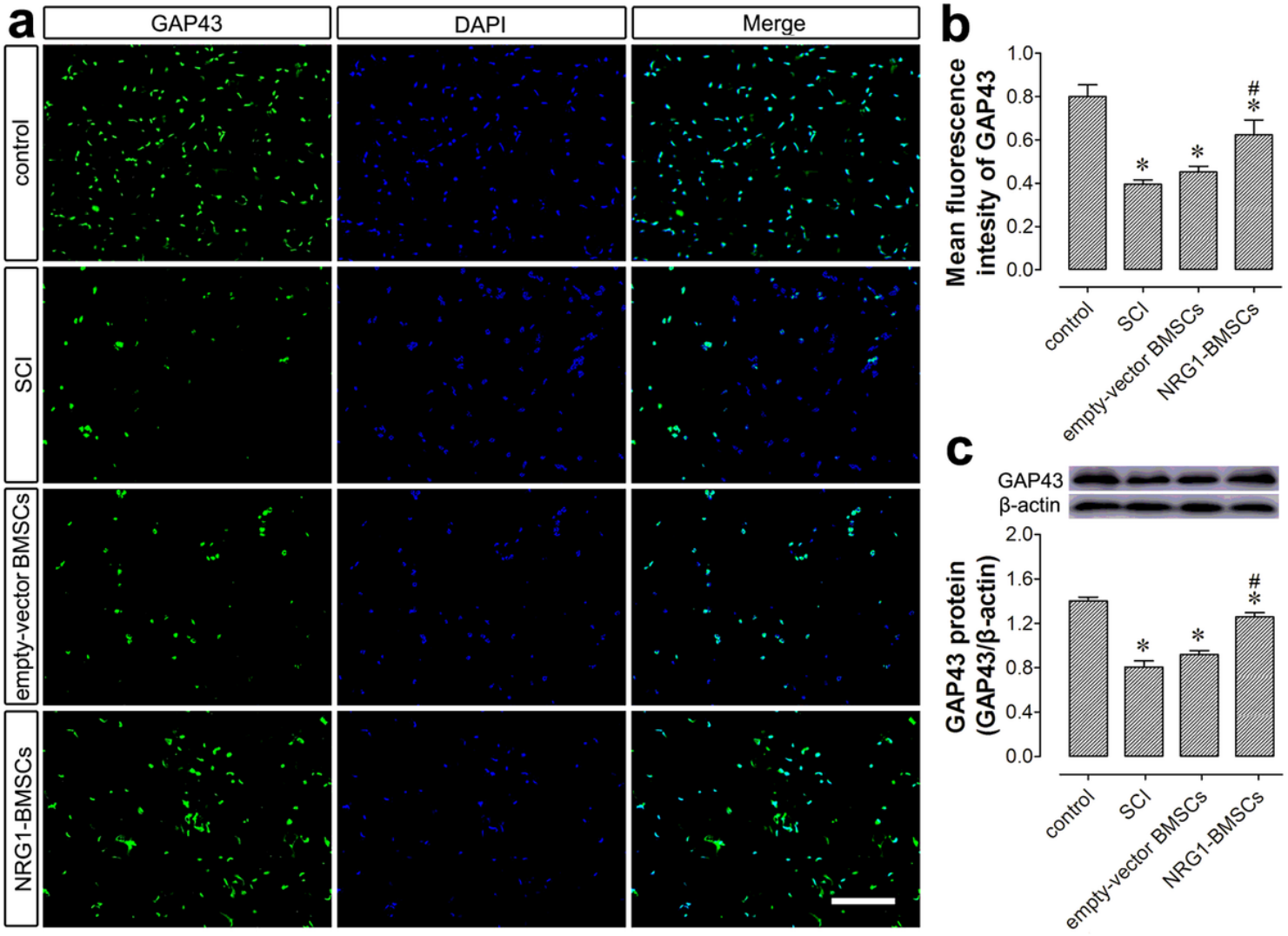

Figure 7

Effects of NRG1-BMSCs on GAP43 expression after SCI. a Representative fluorescent images of GAP43 in spinal cord tissues of the control, SCI, empty-vector BMSCs and NRG1-BMSCs groups. b Quantification of the fluorescence intensity of GAP43 in the control, SCI, empty-vector BMSCs and NRG1-BMSCs groups. c Representative immunoblots (upper) and densitometric analysis (lower) of GAP43 in the control, SCI, empty-vector BMSCs and NRG1-BMSCs groups. Scale bar: 100μm. *P<0.05 vs. control group; #P<0.05 vs. SCI group.

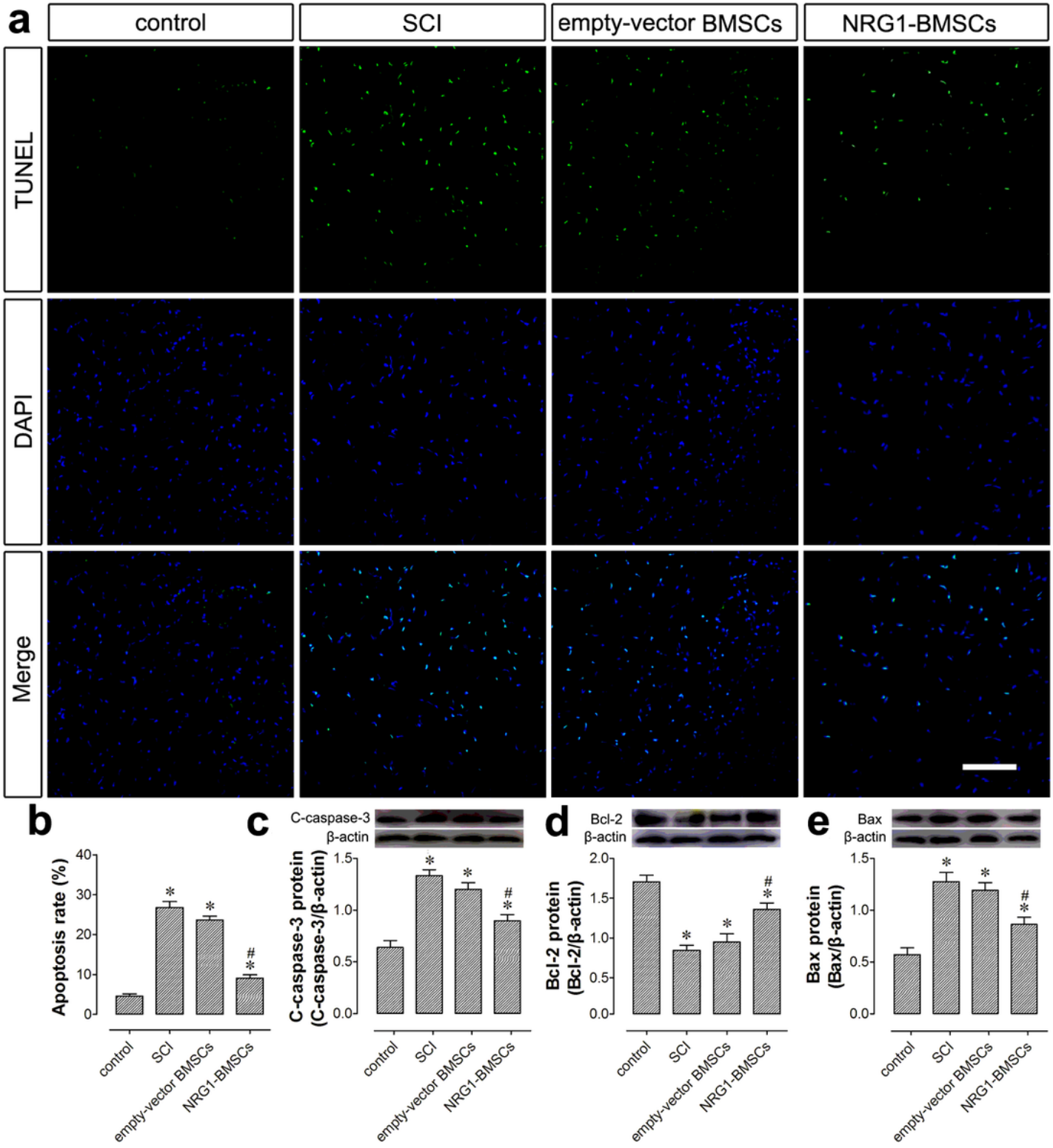

Figure 8

Effects of NRG1-BMSCs on cell apoptosis after SCI. a TUNEL staining of transverse sections of spinal cords from the control, SCI, empty-vector BMSCs and NRG1-BMSCs groups. b Comparison of apoptosis rate of the control, SCI, empty-vector BMSCs and NRG1-BMSCs groups. c-e Representative immunoblots (upper) and densitometric analysis (lower) of cleaved caspase-3, Bcl-2 and Bax protein expressions in the

control, SCI, empty-vector BMSCs and NRG1-BMSCs groups, respectively. Scale bar: 100μm. *P<0.05 vs. control group; #P<0.05 vs. SCI group.